

# Propagation of Cold Pulses and Heat Pulses in ASDEX Upgrade

R. Neu<sup>1</sup>, F. Ryter<sup>1</sup>, R. Dux<sup>1</sup>, H.-U. Fahrbach<sup>1</sup>, A. Jacchia<sup>2</sup>, J.E. Kinsey<sup>3</sup>, F. Leuterer<sup>1</sup>,  
F. De Luca<sup>4</sup>, G. Pereverzev<sup>1</sup>, J. Stober<sup>1</sup>, W. Suttrop<sup>1</sup>, ASDEX Upgrade Team<sup>1</sup>

<sup>1</sup> Max-Planck-Institut für Plasmaphysik, EURATOM Association, Garching, Germany

<sup>2</sup> Istituto di Fisica del Plasma, Associazione EURATOM-ENEA-CNR, Milan, Italy

<sup>3</sup> General Atomics, San Diego, California, United States of America

<sup>4</sup> INFN and Dipartimento di Fisica, Università degli Studi di Milano, Milan, Italy

e-mail: Rudolf.Neu@ipp.mpg.de

**Abstract.** Experiments on electron heat transport were performed in the tokamak ASDEX Upgrade, mainly in ohmically heated plasmas, applying either edge cooling by impurity injection or edge heat pulses with ECH. Repetitive pulses within one plasma discharge were made allowing Fourier transformation of the temperature perturbation. This yields a good signal to noise ratio up to high harmonics and allows a detailed investigation of the pulse propagation. For densities lower than  $1.8 \times 10^{19} \text{ m}^{-3}$ , an increase of the central electron temperature was found as the response to the edge cooling via impurity injection similar to observations made in other tokamaks. The inversion does not appear instantaneously, but with a time delay roughly compatible with diffusion. Modeling of the propagation of the cold pulses in the framework of the IFS-PPPL model yields qualitative agreement. However the predicted increase of the ion temperature is not observed experimentally on the fast time scale. The response to ECH heat pulses is not perfectly symmetrical to cold pulse experiments, but the similarities suggest a common underlying physical mechanism. No inversion of the heat pulse is found, instead the initial pulse from the edge is associated with a second, much slower heat pulse in the centre which is similar (and not symmetrical) to that of the cold pulses. It is found that the central increase is related to the arrival of the pulse close to the inversion radius and not to the initial pulse.

## 1. Introduction

Understanding energy transport in plasmas devoted to fusion research is the subject of intensive studies. A particular observation was made in TEXT, after Laser Blow Off impurity injection (LBO) [1]: the response to the edge cooling was a fast *increase* of the central electron temperature, now known as "non-local" transport with amplitude reversal. Using heat pulses, created by a fast ramp of the plasma current central cooling was observed in TEXT [2]. Further and extensive studies followed these initial observations and more information and references are given in the review paper [3]. Generally, the effect appears at low density, which suggests that it is clearly visible only when electrons and ions are weakly coupled or when  $T_e/T_i$  is large.

## 2. Experimental Set-Up and Methods

Experiments were carried out in the tokamak ASDEX Upgrade ( $R = 1.65 \text{ m}$ ,  $a = 0.5 \text{ m}$ ,  $\kappa \approx 1.6$ ), applying either edge cooling or edge heat pulses. The cold pulses were produced by fast gas puffs and by impurity injection with a repetitive laser ablation system, which allows pulse-rates of up to 20 Hz. Typical amounts of injected particles are a few  $10^{18}$  in the case of C and about  $10^{17}$  in the case of Si and Fe. The heat pulses were launched by Electron Cyclotron Heating (ECH) provided by one 140 GHz gyrotron with about 350 kW of deposited power. The X-mode second harmonic was used, ensuring a narrow ( $< 5 \text{ cm}$ ) single pass absorption of almost 100% (optical depth  $> 3$ ) even close to the plasma edge. Off-axis deposition was achieved by adjusting the magnetic field or/and the launching mirror of the ECH. The electron temperature  $T_e$  is measured by a 60 channel Electron Cyclotron Emission (ECE) heterodyne radiometer with a sampling rate of 31.25 kHz. The optical thickness was sufficient for the measurement of  $T_e$ , at least for radii inside  $\rho_{pol} = 0.9$ . The electron density is gained from a DCN interferometer, covering the main plasma and from a lithium beam diagnostic for the plasma edge.

Using the Fourier method (FFT) to investigate the propagation of repetitive pulses, improves the signal to noise ratio and allows to separate the signal from the modulation caused by the

sawteeth. Based on the assumption of a diffusive transport, the radial profiles of the amplitude and phase of the heat pulses yield the heat diffusivity of the electrons,  $\chi_e^{HP}$  [4,5]. If a convective effect is present, it will be observed *only* on the amplitude profile as an asymmetry which decreases with frequency. Steep gradients of amplitude and phase indicate low transport and flat ones high transport. In our experiments the pulses had a low fundamental frequency (4 to 20 Hz), but produced a large number of harmonics, allowing the investigation over a broad frequency range.

### 3. Propagation of Cold Pulses

Cold pulses were induced, mostly in ohmically heated deuterium plasmas, by injection of C, Si and Fe and also by fast gas puffs with pure deuterium (5 ms duration). Figure 1 shows time traces of the electron temperature from a discharge with  $I_P = 600$  kA and  $B_t = 2.46$  T at  $\bar{n}_e \approx 10^{19}$  m<sup>-3</sup> with a series of cold pulses produced by Fe-LBO. An enhancement of the central  $T_e$  is observed as a reaction to the edge cooling. The central heating does not appear immediately, but its onset is delayed by at least 5 ms, and its maximum occurs 30 ms to 50 ms after the initial pulse (see also Fig. 4). Similar results are obtained by injecting C or Si and stronger edge cooling yields a larger enhancement in the center. Even cold pulses initiated by fast D puffs lead to the same behaviour, indicating that the contribution of the radiation from further inside the plasma is not relevant. In fact, there is a linear relation between the edge cooling and the central heat pulse, independently of the injected element. Figure 2 shows the result of the FFT of the ECE-temperature data for the same discharge. For all harmonics a strong decrease in the amplitude occurs at  $\rho_{pol} \approx 0.5$  correlated with a clear phase jump at the same radial position, the so-called "inversion radius". Since the FFT yields only positive values for the amplitude, the phase jump reflects the inversion of the pulse. Except for the region of the inversion, the amplitude of the perturbation shows a clear *increase* as the pulses propagate towards the centre. This is in contradiction with purely diffusive transport, even apart from the inversion of the sign. However, it cannot be attributed to an inward convection, because it does not decrease with increasing frequency. The effect also cannot be produced on this fast time scale by a rearrangement of the ohmic heating power. Performing cold pulses in discharges with different  $B_t$  and  $I_P$  values, it turned out, that the inversion radius of the cold pulse is always found outside the sawtooth inversion radius. Its position is independent of the strength of the perturbation, of the element injected and also of the electron density. Fig. 3 shows the sawtooth as well as the cold pulse inversion radii versus the edge safety factor ( $q_{95}$ ). Density ramps reveal that the inversion of the cold pulses disappears at line averaged densities  $\bar{n}_e^{max} \approx (1.5 - 1.8) \times 10^{19}$  m<sup>-3</sup>. Using the repetitive injections, it can be clearly demonstrated in a single discharge, that there is no change

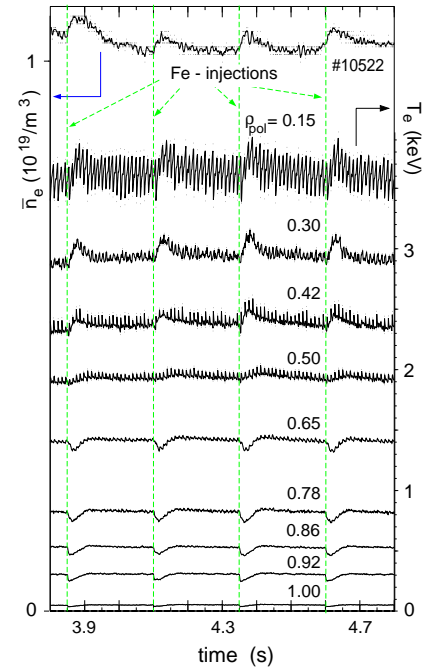


Figure 1:  $T_e$  at different radii showing cold pulses from Fe injection.  $\bar{n}_e$  is shown on the top.

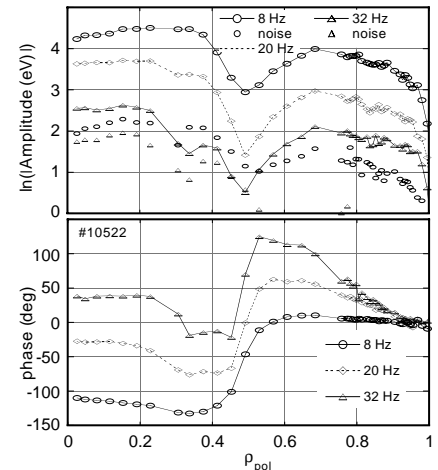


Figure 2: FFT data of discharge 10522 with Fe-LBO cold pulses.

in the inversion radius when approaching  $\bar{n}_e^{max}$ . This is an experimental hint, that the absolute value of  $T_e$  at the inversion radius is not in direct relation to the inversion mechanism.

Looking at  $n_e(0)/\sqrt{T_e(0)} \leq 0.035 \cdot 10^{19} \text{ m}^{-3}/\text{eV}^{1/2}$  as a criterion for the observation of the inversion [6], the maximum value of  $0.040 \cdot 10^{19} \text{ m}^{-3}/\text{eV}^{1/2}$ , found in this work, complies very well. Injections into H-plasmas and He-plasmas showed a similar effect as in D-discharges, as long as the central temperature was high enough to fulfill the criterion.

To interpret the underlying processes, simulations using the IFS-PPPL model [7] – the only model yielding the inversion [8] – were performed. As input for the model the experimental  $n_e$  profile and edge  $T_e$ ,  $T_i$  at  $\rho_{pol} = 0.97$  were used.  $n_e$  is kept constant throughout the calculations. The calculated equilibrium  $T$ -profiles were in good agreement with the experimental ones. The amplitude of the perturbation at the edge was adjusted to match the strength of the central heat pulse. A qualitative agreement with the experiment is obtained and the inversion radius is described rather well, as shown in Fig. 4. It turns out however, that the edge cold pulse has to be assumed much stronger in the modeling and the central heat pulse is too fast compared to the experiment. The essential physics ingredient of the model is a strong  $T_i/T_e$  stabilising effect in the critical gradient. This effect propagates quickly over the radius and a fast enhancement of the ion temperature over the whole radius follows, in reaction to the edge cold pulse [8]. The central increase of the electron temperature is a consequence of the ion behaviour. The predicted rise of the ion temperature ( $\Delta T_i \approx 200 \text{ eV}$ ) should be reflected in an increased neutron rate by a factor larger than two which is not seen in the experiment. The amplitude reversal and the inversion radius on  $T_e$  result from the overlap of the initial cold pulse on the electrons and the increase of  $T_e$  created by the ion behaviour. This explains the S-shaped time evolution of the modeled  $T_e$  at  $\rho_{pol} = 0.50$  (solid line). This behaviour is not observed experimentally and the weak S-shape of the measured  $T_e$  is up-side down compared to the model.

#### 4. Propagation of Heat Pulses

Short heat pulses were produced with ECH at the plasma edge, in discharges with the same parameters ( $I_p$ ,  $B_T$ ,  $\bar{n}_e$ ) as for the cold pulses.  $T_e$  time traces for a discharges with heat edge pulses are shown in Fig. 5. The ECH pulses ( $P_{ECH} \approx 350 \text{ kW}$ ), repeated every 100 ms ( $f = 10 \text{ Hz}$ ), had a duration of 5 ms and were deposited at  $\rho_{pol} \approx 0.85$ . Their shape is inverse of the cold pulses from LBO with good approximation. The channels further inside show that the pulses propagate with decreasing amplitude and become smoother, characteristic of a diffusion-like process. The heat pulses become almost invisible at  $\rho_{pol} \approx 0.4$  and the central channels do not exhibit the clear negative pulses expected from the symmetry with the LBO pulses. At most a very weak decrease of  $T_e$  may be guessed at  $\rho_{pol} \approx 0.29$  and inside. Clearly, the central channels exhibit

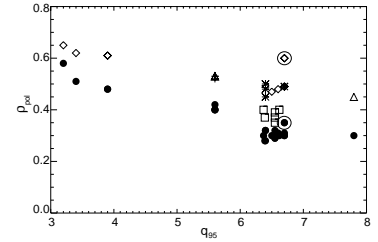


Figure 3:  $q$ -dependence of the sawtooth (●) and the cold pulse inversion radii (+: D, ◇: C, △: Si and \*: Fe), ○: additional central ECH (300 kW, cw), square: inversion radii for the ECH pulses.

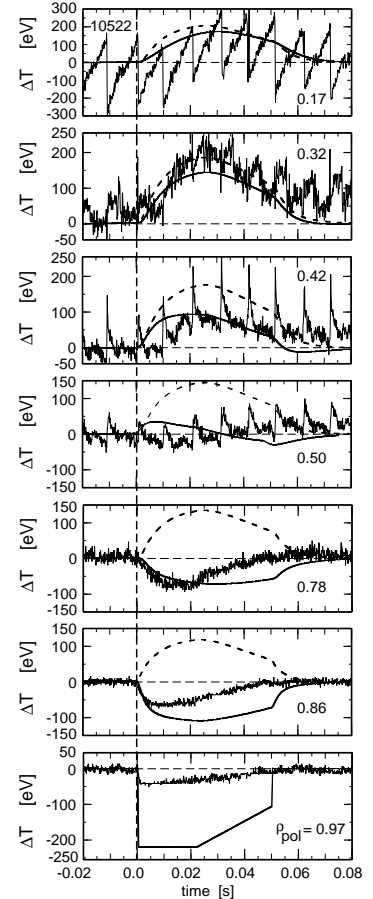


Figure 4: Temporal evolution of  $\Delta T_e$  (—) and  $\Delta T_i$  (- -) from the experiment and the IFS-PPPL-model.

a smooth positive heat pulse with its maximum being delayed by about 30 to 50 ms. The FFT data from discharge # 11162 are given in Fig. 6 for several harmonics up to 50 Hz. They clearly demonstrate the existence of an "inversion radius" at  $\rho_{pol} \approx 0.4$ , where the amplitude strongly decreases and the phase quickly increases. Per analogy with the cold pulses, the term "inversion radius" is also used, although the amplitude does not change sign. Figure 3 shows that the radial position of the inversion radius for ECH pulses is closer to that of the sawteeth than in the cold pulse cases.

The FFT provides additional information: Firstly, the radial location of the ECH deposition at  $\rho_{pol} = 0.83$  is clearly indicated at higher frequencies by the maximum of the amplitude and the minimum of the phase. Secondly, the propagation from the deposition towards the inversion radius is diffusive-like yielding  $\chi_e^{HP} \approx 3 - 5 \text{ m}^2/\text{s}$ , independently of the frequency up to 60 Hz. This value of  $\chi_e^{HP}$  is similar to the value which could be extracted from the phase *only* of the cold pulses. Note, however, the decrease of the amplitude while the pulses propagate inwards, as expected from a diffusive process and in contrast to the LBO pulses. Nevertheless the central response to ECH heat pulses represents a "non-local" character: The FFT data in the central region are not the continuation of the pulse propagation observed up to  $\rho_{pol} = 0.4$ , but the result of a second delayed temperature increase. This delayed pulse seems to have the same amplitude and roughly the same phase over the whole central region and does not show a clear propagating character. Locating the deposition at about mid-radius ( $\rho_{pol} \approx 0.6$ ), the initial ECH pulse is strong enough to be visible on the  $T_e$  time traces in the central region and the initial and the delayed pulse can be clearly separated. The jump in phase at the inversion radius is almost the same for the different positions of deposition. This demonstrates that the reaction of the plasma centre is not directly related to the initial perturbation but rather determined by the arrival of the pulse in the region of the "inversion radius". Additionally, a clear asymmetry of the phase propagation is found. It indicates a lower transport towards the centre ( $\chi_e^{HP} \approx 3 - 5 \text{ m}^2/\text{s}$ ) and a large transport from the ECH deposition towards the edge ( $\chi_e^{HP} \approx 7 - 10 \text{ m}^2/\text{s}$ ), which is quite similar to the propagation of the sawtooth pulses. Discharges with ECH heat pulses at  $\bar{n}_e > 1.5 \times 10^{19} \text{ m}^{-3}$  do not exhibit an "inversion radius".

To quantify the transport changes in the case of the ECH pulses, simulations with the ASTRA transport code [9] were performed. The most important feature of the steady state temperature profile is the change of slope around  $\rho_{tor} = 0.4$ , which requires a low  $\chi_e$  value in the centre. A heat pinch, which would also be able to cause the central peaking, is excluded by the experimental modulation results presented above. Simulating the ECH pulses yields a  $\chi_e^{HP} \approx 3 - 5 \text{ m}^2/\text{s}$  for pulse propagation towards the centre and also a strong reduction around  $\rho_{tor} = 0.4$ . This step provides the decrease of the amplitude and the variation of the phase as the pulses approach the inversion radius, but it is not sufficient to reproduce the increase of

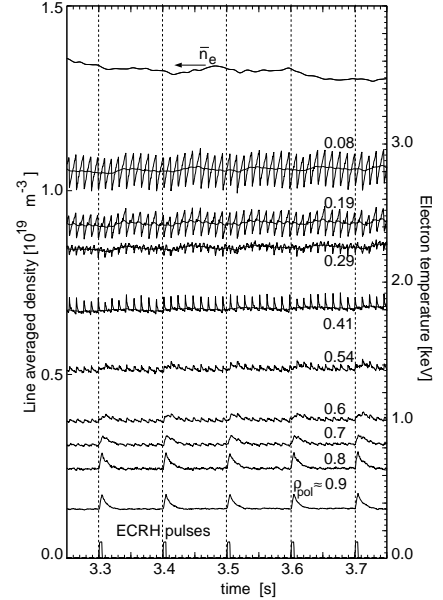


Figure 5:  $T_e$  at different radii showing ECH heat pulses.

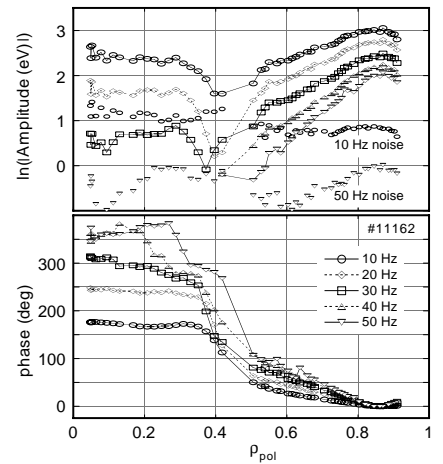


Figure 6: FFT data of discharge 11162 with ECH heat pulses.

the central  $T_e$  following the edge heat pulse with the time delay of 30 ms. For this purpose a time dependence is necessary and  $\chi_e$  is modulated in time by *only* 15%, in the central region. Although this procedure does not provide any physical explanation, it demonstrates that a *small* change in  $\chi_e$  is sufficient to explain the observations, making the underlying physics difficult to identify. It was also attempted to simulate the ECH heat pulses using the IFS-PPPL model. As expected, the experimental observation cannot be reproduced by the model, because it provides an inversion of the temperature perturbation. There is also no experimental indication of any decrease of the neutron emission rate as predicted by the ITG model.

## 5. Discussion

The cold pulses as well as the heat pulses exhibit a comparable temperature increase which occurs on the same slow time scale. This similarity suggests a common underlying physical mechanism which changes transport in the same manner around and inside the inversion radius. The different behaviour outside the inversion radius may result from the following: The ECH pulses do not create any density change whereas the cold pulses are caused and accompanied by a particle source and energy sink. Therefore cold pulses affect both, ions and electrons whereas ECH pulses heat exclusively the electrons. Especially the difference in the behaviour of the amplitude of the perturbation may be due to the interaction with ions, or caused by the some combination of energy and particle transport. In the region inside the inversion radius, the following common properties of cold and heat pulses are evident: The central temperature increase is related to the arrival of the initial perturbation close to the inversion radius and the time delay of the central temperature increase is comparable. The central "non-local" reaction occurs only below the same limit in density and the amplitude in the centre is proportional to that of the initial perturbation at the edge.

Our study suggests the existence of different transport mechanisms inside and outside of the "inversion radius". Outside, transport seems to be governed by critical gradient physics for the electrons at least, as shown by the pulse propagation and in particular by the phase asymmetry. Inside the inversion radius, transport is low as indicated by the required step in  $\chi_e$ . One may link the low transport in the inner region with the weak shear sustained by the sawtooth activity. In such a situation with two radial regions dominated each by different transport mechanisms, one may imagine that the arrival of cold or heat pulses at the transition zone is able to slightly modify the transport at least in the inner region and causes the observed effect.

## Acknowledgement

We are glad to thank P. Mantica and A.G. Peeters for stimulating discussions, and W. Dorland for having kindly given us the routine of the IFS-PPPL model. The modeling of the cold pulses with the IFS-PPPL model by J. Kinsey was partly supported by DOE contract Grant No. DE-FG03-95ER54309.

## References

- [1] GENTLE, K.W., et al., *Phys. Rev. Lett.* **74**, (1995) 3620.
- [2] GENTLE, K.W., et al., *Phys. Plasmas* **4**, (1997) 3599.
- [3] CALLEN, J.D. and KISSICK M.W., *Plasma Phys. Contr. Fusion* **39**, (1997) B173.
- [4] LOPES CARDOZO, N.J., *Plasma Phys. Contr. Fusion* **37**, (1995) 799 and ref. therein.
- [5] JACCHIA, A., et al., *Phys. Fluids B* **3**, (1991) 3033.
- [6] KISSICK M.W., et al., *Nucl. Fusion* **38**, (1998) 821.
- [7] KOTSCHENREUTHER, M., et al., *Phys. Plasmas* **2**, (1995) 2381.
- [8] KINSEY, J.E., et al., *Phys. Plasmas* **5**, (1998) 3974.
- [9] PEREVERZEV, G.V., et al., *Report 5/42 MPI für Plasmaphysik, Garching (1991)*.